Women and girls continue to bear disproportionate impacts of heatwaves in South Sudan that have become a constant threat

Authors

Sarah Kew, *Royal Netherlands Meteorological Institute (KNMI), De Bilt, The Netherlands*
Izidine Pinto, *Royal Netherlands Meteorological Institute (KNMI), De Bilt, The Netherlands*
Sjoukje Philip, *Royal Netherlands Meteorological Institute (KNMI), De Bilt, The Netherlands*
Joyce Kimutai, *Centre for Environmental Policy, Imperial College, London, UK*
Maja Vahlberg, *Red Cross Red Crescent Climate Centre, The Hague, the Netherlands; Swedish Red Cross, Stockholm, Sweden (based in Ubmeje/Umeå, Sweden)*
Roop Singh, *Red Cross Red Crescent Climate Centre, The Hague, the Netherlands (based in New Jersey, USA)*
Kiswendsida Guigma, *Red Cross Red Crescent Climate Centre, The Hague, the Netherlands (based in Ouagadougou, Burkina Faso)*
Karina Izquierdo, *Red Cross Red Crescent Climate Centre, The Hague, the Netherlands (based in Mexico City, Mexico)*
Lisa Thalheimer, *International Institute for Applied Systems Analysis, Laxenburg, Austria*
Martha M. Vogel, *Red Cross Red Crescent Climate Centre, The Hague, the Netherlands (based in Zurich, Switzerland)*
Nick Baumgart, *Copenhagen Centre for Disaster Research, Global Health Section, Department of Public Health, University of Copenhagen, Copenhagen, Denmark*
Emmanuel Raju, *Copenhagen Centre for Disaster Research, Global Health Section, Department of Public Health, University of Copenhagen, Copenhagen, Denmark; AND African Centre for Disaster Studies, North-West University, South Africa*
Friederike Otto, *Centre for Environmental Policy, Imperial College, London, UK*

Review authors

Mariam Zachariah, *Centre for Environmental Policy, Imperial College, London, UK*
Shaban Mawanda, *Red Cross Red Crescent Climate Centre, The Hague, the Netherlands (based in Kampala, Uganda)*
Marcel Goyeneche, *Red Cross Red Crescent Climate Centre, The Hague, the Netherlands (based in Santiago, Chile)*
Madeleine Lundberg, *Swedish Red Cross, Stockholm, Sweden*

Main findings

- In South Sudan, gender plays a crucial role in shaping vulnerability, exposure, and coping capacity to extreme heat events. Women in the country face huge challenges, including high maternal mortality (1,223 women per 100,000 live births), lower adult literacy (29% compared to 40% for men), and are only represented with 32% of the seats in national parliament. Almost all women that have employment are working in the informal sector (95%).
- Women predominantly work in agriculture (or another occupation with high heat exposure, such as street vending or manufacturing) and spend 60% of their time on unpaid care work, such as fetching water, and cooking in extremely hot environments. This sustained heat exposure with physical exertion can have serious long-term health effects, including cardiovascular strain, kidney damage, and increased vulnerability to heat exhaustion and heat stroke.
- Education is severely impacted by extreme heat. Prolonged school closures increase the likelihood of learning losses, reinforce gendered household expectations, and heighten risks of early marriage, making school return more difficult for girls. Actions such as changing the timing of school to avoid the hottest part of the day, or rearranging the academic calendar, suggested by education workers could help avoid long-term closures. Retrofitting school buildings with passive cooling options (e.g. shade trees, painting roofs white) can also be a low-cost way of reducing risks, along with first aid education for teachers and students to recognise the signs of heat-related illness and take appropriate action.
- Malnutrition, already affecting 860,000 children under five in South Sudan, is worsened by extreme heat. Extreme heat worsens food insecurity, weakens immune systems, and increases the risk of dehydration and illness, particularly in children in female-headed households. Limited access to food, healthcare, and income security compounds these vulnerabilities, creating a cycle of worsening health outcomes and deepening inequalities.
- Displacement and conflict heighten heat risks, particularly for women and girls. Armed conflict in the region has forced over 1.1 million people into overcrowded shelters with poor ventilation, worsening heat exposure. Displaced women often lack access to cooling, water, and healthcare and are at heightened risk of violence.
- The hottest temperatures of the year are not usually expected to occur as early as February when this extreme heat was observed. In today's climate however, which has warmed by 1.3C, the 7-day nighttime and daytime temperatures observed in the South Sudan region are no longer unusual even for February.
- However, the 7-day maximum heat in the South Sudan region would have been extremely unusual in a 1.3C colder climate, if the world had not warmed due to the burning of fossil fuels. Based on observations, extreme heat such as observed in 2025 would have been extremely unlikely to occur in a 1.3C colder climate. A similarly frequent 7-day heat event would have been around 4C cooler in a 1.3C cooler climate.
- When combining the observation-based analysis with climate models, to quantify the role of climate change in this 7-day heat event, we find that climate models underestimate the increase in heat found in observations. We can thus only give a conservative estimate of the influence of human-induced climate change. Based on the combined analysis we conclude that climate change made the extreme heat at least 2C hotter and at least 10 times more likely.

- Due to the known deficiencies in climate models to represent extreme heat, estimating future changes in the 7-day maximum heat over the South Sudan region also only allows us to give very conservative estimates. At a global warming of 2.6C the likelihood and intensity of such events continue to increase.
- While large-scale adaptation remains a challenge, targeted interventions can help communities manage heat risks even in difficult situations and conflict-torn regions. Expanding access to safe water, shaded areas, and cooling spaces - especially in displacement camps and informal settlements - can offer relief. Ajuong Thok refugee camp which shelters over 40,000 people, most of whom are women, is a positive example of better shelter design in this region.
- Adaptation strategies must be designed with conflict and gender considerations in mind to avoid reinforcing existing inequalities. Supporting women farmers with climate-resilient agricultural practices, strengthening labor protections for outdoor workers, and providing financial assistance to vulnerable households can help build coping capacity. Impact-based early warnings are already in development by IGAD, the regional centre, and will be critical for improving preparedness, but last-mile dissemination of warnings and impacts are critical to ensuring that people take lifesaving, self-protective actions.

1 Introduction

In February 2025, extreme temperatures swept across several regions of East Africa (ICPAC[1], 2025). The Intergovernmental Authority on Development (IGAD) Climate Prediction and Application Centre ICPAC's forecast, released on February 21, 2025, had indicated that above-average temperatures would impact several areas, including Eastern Kenya, South Sudan, Eastern Tanzania, Southern Sudan, and Southern Somalia. According to this forecast, most parts of Southern Sudan have been expected to experience 7-day averaged mean temperatures exceeding 32°C, and the greater Horn of Africa, including parts of Kenya and Somalia to expect temperatures ranging from 20-32°C (Somali Magazine). Further, elevated heat stress levels are expected in most parts of South Sudan, eastern parts of Tanzania, parts of southern Sudan, eastern Kenya and southern Somalia. In South Sudan, intense heat during mid-to-late February forced schools to close for two weeks after students collapsed from heat exhaustion and heat stroke (AP News, 2024). Temperatures are expected to remain above normal over most parts of South Sudan in March (ICPAC, 2025). In Kenya, the Meteorological Department also issued an advisory, predicting sunny, dry, and hot weather conditions over most parts of the country in the last week of February going into the 1st week of March (KMD, 2025). Cooler conditions are expected in Northern Sudan, the Ethiopian highlands, and Central and Western Kenya.

Previous studies show that temperatures in most parts of the subtropics and tropical Africa have been increasing at more than twice the global average rate (Engelbrecht et al., 2015; Trisos et al., 2022), with temperatures frequently exceeding the upper limit of human comfort (Sherwood & Huber, 2010; Iyakaremye et al., 2021). The increase in hot extremes over East Africa has been unequivocally linked to human-induced warming resulting from cumulative greenhouse concentrations in the atmosphere since the pre-industrial period (IPCC, 2021). As the climate continues to warm, the frequency and intensity of heatwaves are expected to further increase, posing significant health risks to populations.

[1] IGAD (Intergovernmental Authority on Development) Climate Prediction Centre

Demissie et al. (2025) found that the frequency of hot spells, as well as the duration and intensity of heatwaves, are projected to increase in the region in the future. Heat-related health impacts have become a public health challenge, with studies demonstrating a direct relationship between rising temperatures and an increase in hospital emergency visits, admissions and fatalities (Kunda et al., 2024; Kimutai et al., 2022). In Africa, heat events and heat-health impacts are often underreported in extreme weather and impacts databases e.g. EMDAT, and many national meteorological services lack heat early warning systems (Harrington & Otto, 2020; Kimutai et al., 2022). Future climate projections indicate that by mid-century, 19-45% of days in parts of East Africa will be classified as 'hot days.' Additionally, 45-75% of nights are expected to be 'hot nights,' a figure that could rise to 64-93% by the end of the century (World Bank, 2021). Like many cities in the Global South, African cities are experiencing rapid urbanization leading to the expansion of highly vulnerable urban communities in informal settlements, often located in regions highly susceptible to extreme weather events. Many of these informal settlements lack essential infrastructure and services such as cooling infrastructure, green spaces, or shelters, making them highly vulnerable to extreme heat. This, in turn, places significant strain on civic infrastructure as demand for essential services continues to rise.

Extreme heat is often associated with significant shifts in atmospheric circulation and precipitation patterns, as well as changes in land and ocean surface conditions (Luo & Lau, 2017). In East Africa, where a complex interaction of local factors such as topography, mesoscale systems and large-scale circulation plays a crucial role in temperature and rainfall variability, previous studies suggest that anticyclonic anomalies over the region are key drivers of extreme heat events (e.,g Hu et al;, 2019). In such cases, the air temperature rises due to a combination of adiabatic heating and enhanced solar radiation at the surface, both of which result from subsidence linked to the anomalous anticyclonic system and concurrent anomalous convergence in the upper troposphere. The intensification of the Arabian high pressure system (at low level) during northern spring (MAM season over East Africa) is known to trigger strong northerly flow transporting heat into the region while subsequently displacing the ITCZ (InterTropical Convergence Zone) (Lashkari & Jafari, 2021; Okoola, 1999). While wind flows are not depicted, Figure 1.1 illustrates similar conditions, showing the intensification of the Arabian High during periods of elevated temperatures in the region.

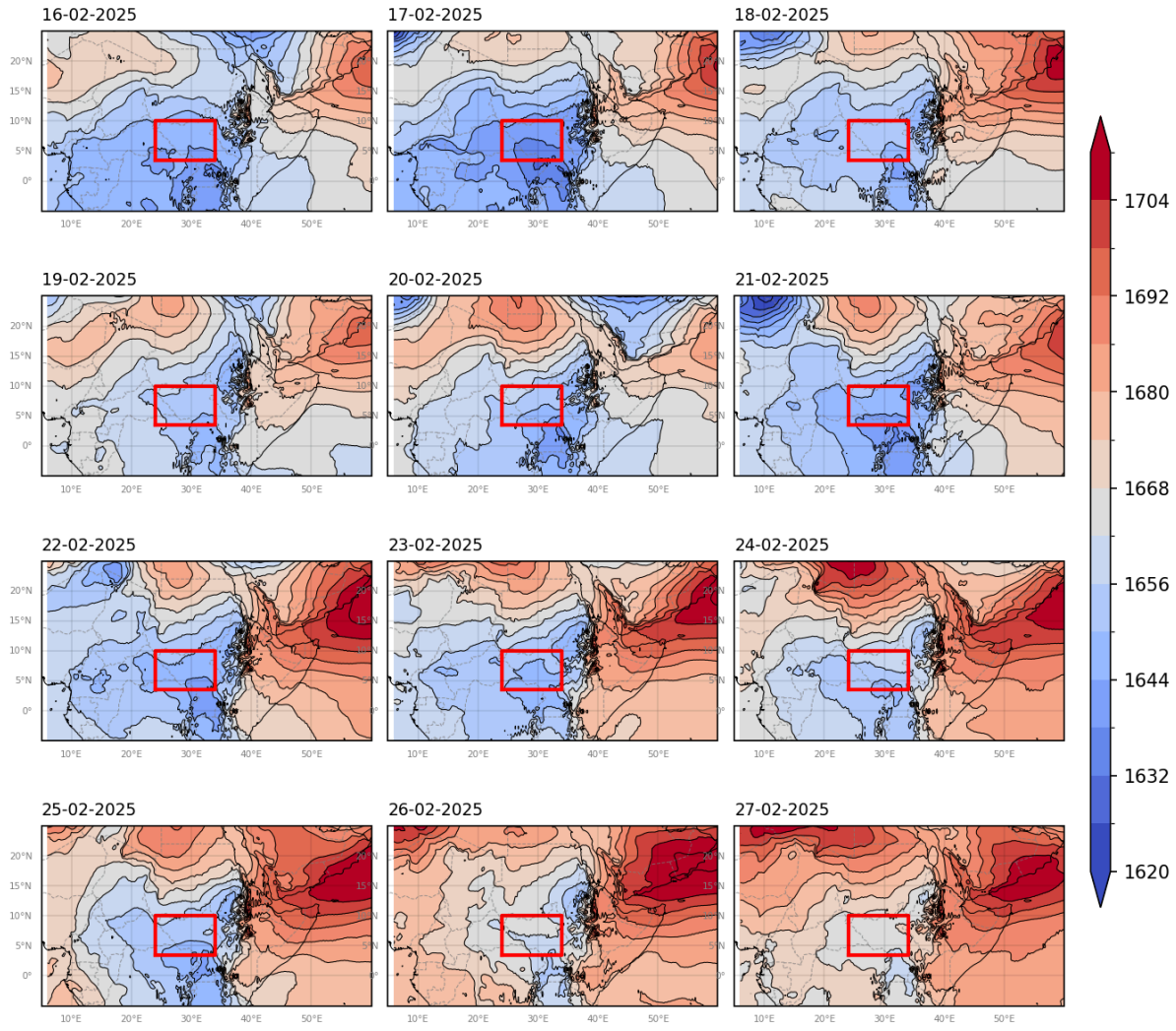

Figure 1.1. Mean daily Geopotential heights [m] at 850hPa depicting the circulation (5°E to 62°E; 5°S to 26°N) over the days of high temperatures. The box shows the study region. Borders shown are generated using a standard plotting package and do not imply official endorsement nor political opinion on included territories. Source: ERA5.

1.2 Event Definition

To define the event, we use the July-June maximum of 7-day running mean daily maximum temperature (TX7x), averaged over a box area compassing South Sudan with coordinates 24°E to 34°E; 3.5°N to 10°N (Figure 1.2). Note that where borders are shown in maps in this report, we used a standard package and they do not imply official endorsement or political stance on any depicted territories. These borders are not used in any analyses.

In the analysis of the event, we utilise ERA5 reanalysis data to analyse maximum and minimum temperatures over the same region and for the same temporal definition (TN7x). We acknowledge that humidity is an important factor in the impacts of heat events over South Sudan and the entire region. While an index such as the heat index that incorporates humidity is more relevant for understanding humid heatwaves, trends in maximum and minimum temperatures can still offer valuable insights into

the potential impacts on ecosystems and human health. For this rapid study, we choose to only look at the temperatures.

In this report, we study the influence of anthropogenic climate change by comparing the likelihood and intensity of similar TX7x events in the present climate with those in a 1.3 °C cooler climate. We also extend this analysis into the future by assessing the influence of a further 1.3 °C of global warming from present. This is in line with the latest Emissions Gap Report from the United Nations Environment Programme, which shows that the world is on track for at least 2.6 °C temperature rise given currently implemented policies (UNEP, 2024).

This document is intended as a short, super-rapid attribution report on the heatwave, with a more concise hazard analysis as compared to regular World Weather Attribution studies. The event definition uses a standard index over a longitude-latitude rectangular domain and is less tailored to impacts. A single gridded observational dataset (ERA5) and one multi-model ensemble (CMIP6) is used. No local observational datasets are included. Standard methods are used as in regular studies and the analysis on Vulnerability and Exposure is regular.

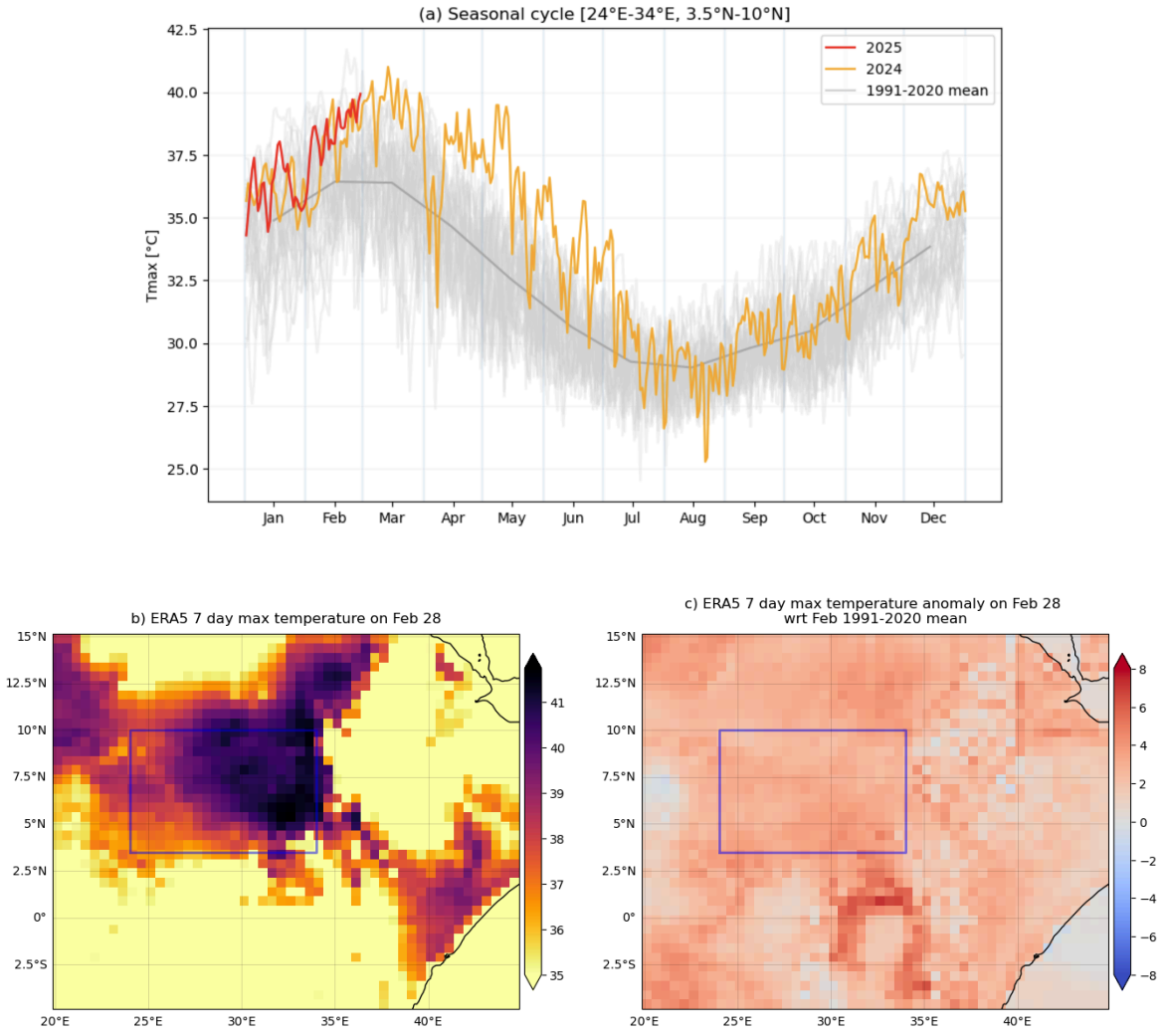

Figure 1.2. Daily variability of maximum temperature over the study region (a), seven day average maximum temperature (TX7x) for the period of 20 of February to 27 of February (b) and TX7x anomaly with respect to February climatology over the period of 1991-2020. Data ERA5.

2 Data and methods

2.1 Observational data

The European Centre for Medium-Range Weather Forecasts's 5th generation reanalysis product, ERA5, is a gridded dataset that combines historical observations into global estimates using advanced modelling and data assimilation systems (Hersbach et al., 2020). We use maximum temperature and minimum temperature data from this product at a resolution of 0.25°x0.25°. The re-analysis is available from 1940 until the end of January 2025. We extend the re-analysis data with the ECMWF analysis to cover the whole month of February 2025. Data before 1970 has however not been used due to irregularities in the reanalysis data that are not apparent in the station data that is available for South Sudan.

As a measure of anthropogenic climate change we use the (low-pass filtered) global mean surface temperature (GMST), where GMST is taken from the National Aeronautics and Space Administration (NASA) Goddard Institute for Space Science (GISS) surface temperature analysis (GISTEMP, Hansen et al., 2010 and Lenssen et al. 2019).

2.2 Model and experiment descriptions

In this super-rapid analysis, we use just one coupled global circulation model ensemble, CMIP6, in contrast to a full analysis where more than one climate modelling experiment would be considered from different framings (Philip et al., 2020). This consists of simulations from 17 participating models with varying resolutions. For more details on CMIP6, please see Eyring et al., (2016). For all simulations used here, the period 1850 to 2015 is based on historical simulations, while the SSP5-8.5 scenario is used for the remainder of the 21st century. Only one ensemble member from each model is analysed for TX7x. Each model's GMST is used as co-variate, smoothed with a 4-year running mean.

2.3 Statistical methods

Methods for observational and model analysis and for model evaluation and synthesis are used according to the World Weather Attribution Protocol, described in Philip et al., (2020), with supporting details found in van Oldenborgh et al., (2021), Ciavarella et al., (2021), Otto et al., (2024) and here. The key steps, presented in sections 3-6, are: (3) trend estimation from observations; (4) model validation; (5) multi-method multi-model attribution; and (6) synthesis of the attribution statement.

In this report we analyse the time series of TX7x over a box area over South Sudan. A nonstationary GEV distribution is used to model TX7x. The distribution is assumed to shift linearly with the covariates and the variance to remain constant. The parameters of the statistical model are estimated using maximum likelihood.

For each time series we calculate the return period and intensity of the event under study for the 2024 GMST and for 1.3 °C cooler GMST: this allows us to compare the climate of now and of the preindustrial past (1850-1900, based on the Global Warming Index), by calculating the probability ratio (PR; the factor-change in the event's probability) and change in intensity of the event. In addition to that, for model data we analyse a 1.3 °C warmer climate.

3 Observational analysis: return period and trend

Using ERA5 analysis data over February 2025, the magnitude of the TX7x event (22-28 February 2025) averaged over the box is 39.3 ℃. Locally, the TX7x exceeds 42°C for a small area in the upper right part of the study area. We note however that more heat has been forecasted for the first days of March 2025. Therefore the event magnitude and with this the return period, might be a slight underestimation. Since the school closure has been announced based on the higher than normal temperatures of the end February, the current event magnitude and return period (see below) are relevant for the analysis. Results in this analysis do not depend much on the exact return period.

Using ERA5 reanalysis and analysis data from 1970 to the end of February 2025 and a GEV that shifts with the smoothed GMST, we calculate for TX7x the return period in the current climate, change in intensity and probability ratio between the 2024/25 climate and a past climate that is 1.3 ℃ cooler than now (i.e. without anthropogenic warming), see Figure 3.1. The return period is estimated to be about 2 years (95% CI 1.4 to 3 years). This means that such an event such as the one that happened at the end of February 2025 is nowadays rather normal. Due to the large trend the probability ratio is quite large too, with an undefined upper bound and a best estimate of 893 and a lower bound of 55. The change in intensity is quite large: 4.0 ℃ (95% CI 3.1 ℃ to 4.7 ℃). For the model analysis we use a return period of 2 years. A spatial analysis of the change in intensity over the wider region (figure 3.3) shows that the intensity change is quite uniform over South Sudan, equally high in regions southwest of South Sudan but less strong elsewhere in the region.

In addition to the analysis of maximum temperatures, we also include an analysis of minimum temperatures in ERA5, see figure 3.2. We note however that the maximum of minimum temperatures over the South Sudan region normally peaks in March/April, so the current heat event does not happen at the peak of the seasonal cycle for minimum temperature. As a consequence, the return period of the current TN7x event is likely not representative of this year's maximum value. In the GEV analysis this does not have an influence on the change in intensity (due to the linear shift of the GEV distribution with GMST, the intensity change between the two evaluated climates is the same for all return periods or event magnitudes), and only a small influence on the probability ratio (the shape parameter is only slightly negative, behaving almost like a Gumbel - exponential decay which is linear on the log-scale return period figure - but with a slightly shorter tail, with the consequence that there is only a slight increase in PR as event magnitude increases). Therefore, for TN7x we emphasize the trend and not the return period of the last 7 days of February (current TN7x magnitude). Also for

TN7x, due to the large trend, the probability ratio is quite large too, with an undefined upper bound and a best estimate of 59.6 and a lower bound of 11.4. The change in intensity is quite large: 2.9 ℃ (95% CI 1.9 ℃ to 3.9 ℃).

With respect to the July to June TN7x for all other years, the TN7x for 2024/2025 (14th-20th February) is not at all extreme for the current climate - actually being well below average for the current climate - but would have been very extreme for the past climate that is 1.3°C cooler than now. If the same GEV analysis is repeated for the month of February only (not shown), the 2025 value is still not extreme, being slightly below average for the current climate with a return period of 1.4 years.

The minimum temperatures were not a distinguishing feature of this heat episode or its impacts and are therefore not studied further with models.

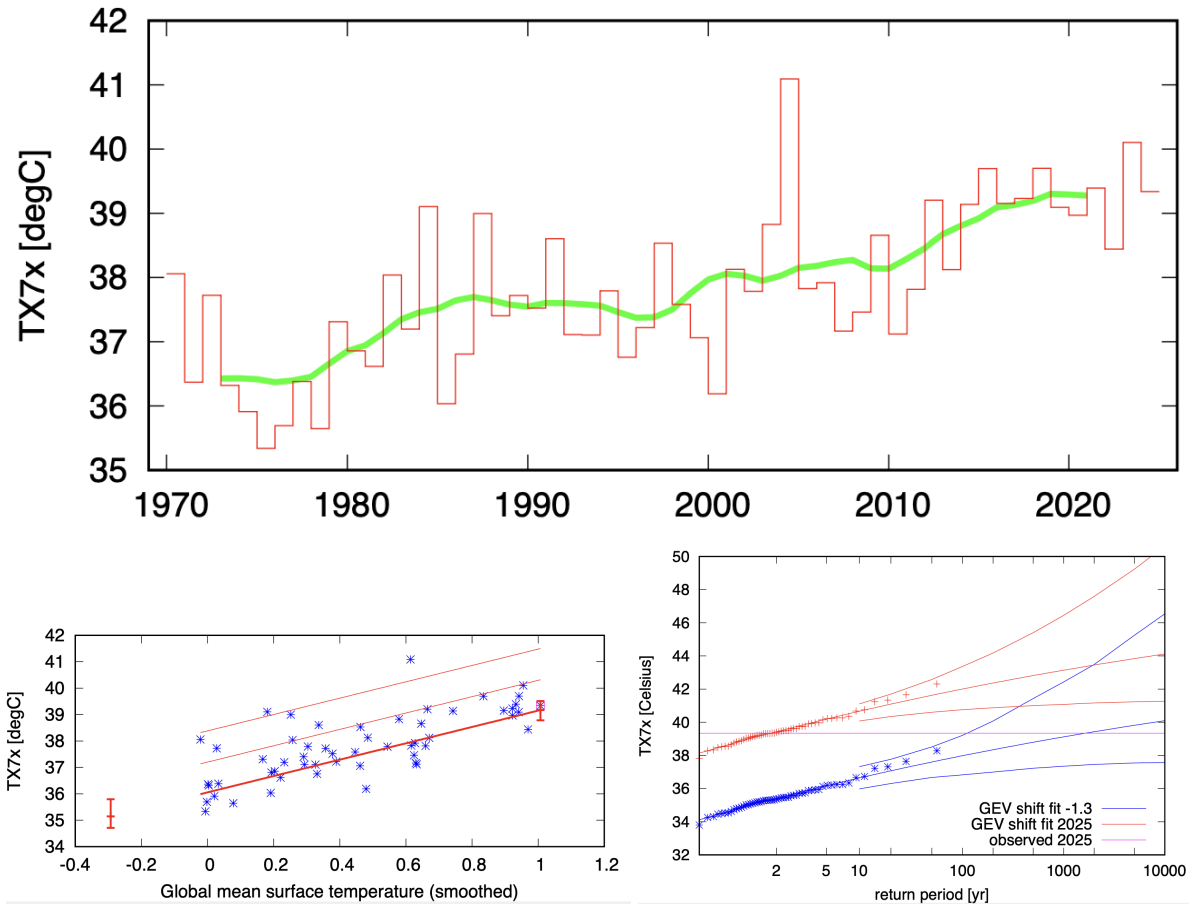

Figure 3.1 Top: Time series of TX7x along with the 10-year running mean (green line). Bottom left: TX7x over the study region estimated from ERA5 records to change in global mean temperature. The thick red line denotes the time-varying mean, and the thin red lines show 1 standard deviation (s.d) and 2 s.d above. The vertical red lines show the 95% confidence interval for the location parameter, for the current, 2024/25 climate and the hypothetical, 1.3ºC cooler climate. The February 2025 observation is highlighted with the magenta box. Bottom right: Return periods for the 2024/25 climate (red lines) and the 1.3ºC cooler climate (blue lines with 95% CI), based on ERA5 data.

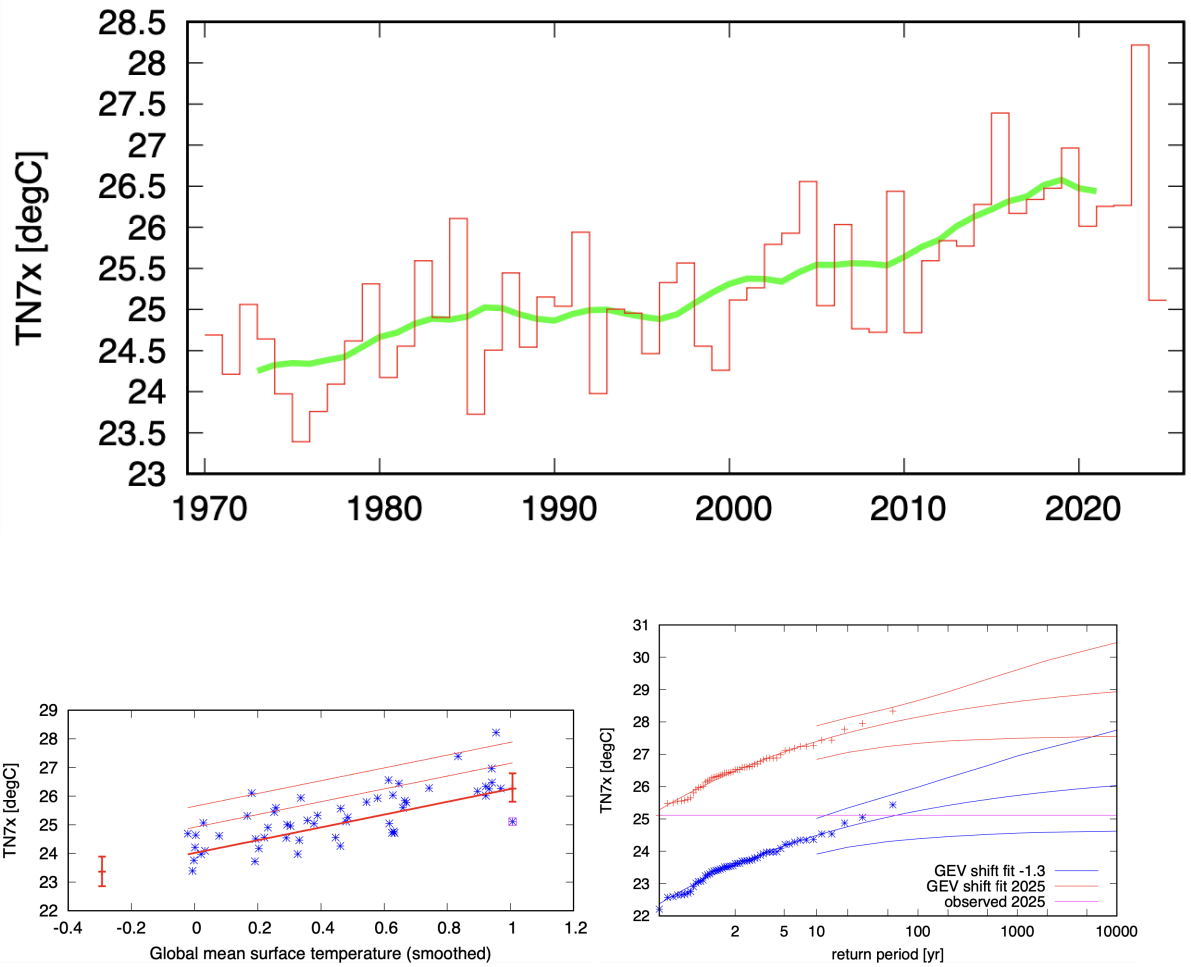

Figure 3.2. Same as Figure 3.1 but for TN7x.

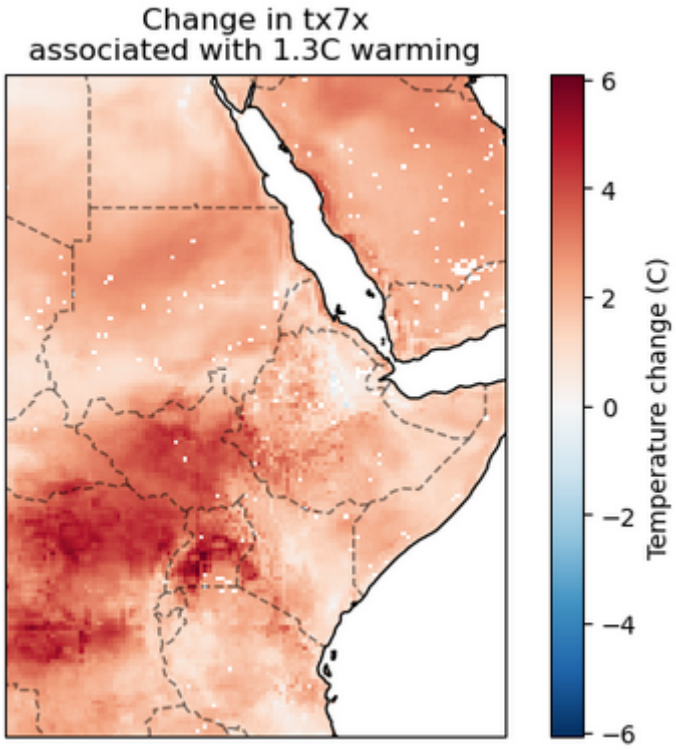

Figure 3.3. Map of expected change in intensity of TX7x events in response to a 1.3C increase in GMST, under a GEV model that shifts with GMST. Borders shown are generated using a standard plotting package and do not imply official endorsement nor political opinion on included territories. Source ERA5.

4 Model evaluation

In this section we show the results of the model evaluation for the assessed region. The climate models are evaluated against the observations in their ability to capture:

1. Seasonal cycles: For this, we qualitatively compare the seasonal cycles based on model outputs against observations-based cycles. We discard the models that exhibit ill-defined peaks in their seasonal cycles. We also discard the model if the hot season onset/termination varies significantly from the observations.

2. Spatial patterns: Models that do not match the observations in terms of the large-scale annual mean temperature patterns are excluded.

3. Parameters of the fitted statistical models. We discard the model if the model and observation parameters ranges do not overlap.

The models are labelled as ‘good’,’reasonable’, or ’bad’ based on their performances in terms of the three criteria discussed above. A model is given an overall rating of ‘good’ if it is rated ‘good’ for all three characteristics. If there is at least one ‘reasonable’, then its overall rating will be ‘reasonable’ and ‘bad’ if there is at least one ‘bad’.

Per framing or model setup we only use models that only pass the validation tests with the label 'good' as this results in using 9 models that perform well. The tables show the model validation results.

Table 4.1 Evaluation results of the climate models considered for attribution analysis of TX7x. For each model, the threshold for a 1-in-2-year event is shown, along with the best estimates of the Sigma and Shape parameters are shown, along with a 95% confidence intervals. Furthermore evaluation of the seasonal cycle and spatial pattern are shown. Models with label 'good' that are used in the analysis are colored green.

Model / Observations	**Seasonal cycle**	**Spatial pattern**	**Sigma**	**Shape parameter**	**Conclusion**
ERA5			0.711 (0.517 ... 0.860)	-0.064 (-0.30 ... 0.15)	
ACCESS-CM2	good	good	0.680 (0.490 ... 0.810)	-0.24 (-0.41 ... -0.060)	good
ACCESS-ESM1-5	good	good	0.700 (0.530 ... 0.850)	-0.41 (-0.65 ... -0.20)	reasonable
CanESM5	good	good	0.750 (0.670 ... 0.670)	-0.52 (-0.47 ... -0.47)	bad
CMCC-ESM2	good	good	0.580 (0.440 ... 0.750)	-0.090 (-0.47 ... 0.14)	good
CNRM-CM6-1-HR	bad	good	0.890 (0.660 ... 1.14)	-0.33 (-0.95 ... -0.060)	reasonable
CNRM-CM6-1	bad	good	0.920 (0.740 ... 1.05)	-0.51 (-0.72 ... -0.31)	bad
EC-Earth3	good	good	0.700 (0.540 ... 0.810)	-0.20 (-0.42 ... -0.020)	good
EC-Earth3-Veg	good	good	0.700 (0.550 ... 0.860)	-0.16 (-0.35 ... 0.10)	good
EC-Earth3-Veg-LR	good	good	0.670 (0.540 ... 0.820)	-0.19 (-0.52 ... -0.020)	good
FGOALS-g3	good	good	0.670 (0.530 ... 0.800)	-0.24 (-0.59 ... -0.10)	good
INM-CM4-8	good	good	0.520 (0.380 ... 0.630)	-0.25 (-0.50 ... 0.0)	good
INM-CM5-0	good	good	0.610 (0.540 ... 0.620)	-0.49 (-0.63 ... -0.42)	bad
MIROC6	good	good	1.14 (0.910 ... 1.31)	-0.11 (-0.25 ... 0.10)	bad
MPI-ESM1-2-HR	good	good	0.780 (0.590 ... 0.930)	-0.18 (-0.52 ... -0.040)	good
MPI-ESM1-2-LR	good	good	0.770 (0.620 ... 0.920)	-0.33 (-0.78 ... -0.11)	reasonable
MRI-ESM2-0	reasonable	good	0.990 (0.740 ... 1.17)	-0.29 (-0.56 ... -0.080)	reasonable
NorESM2-MM	good	good	0.750 (0.540 ... 0.920)	-0.22 (-0.50 ... 0.030)	good

5 Multi-method multi-model attribution

This section shows Probability Ratios and change in intensity ΔI for models that passed model evaluation and also includes the values calculated from the fits with observations.

Table 5.1. Event magnitude, probability ratio and change in intensity for 2-year return period for TX7x for observational datasets and each model that passed the evaluation tests. (a) from pre-industrial climate to the present and (b) from the present to 2.6℃ above pre-industrial climate

Model / Observations	**Threshold for return period 2 yr**	**Probability ratio PR [-]**	**Change in intensity ΔI [˚C]**	**Probability ratio PR [-]**	**Change in intensity ΔI [˚C]**
		Past - Present		**Present - Future**	
ERA5	39.338 ˚C	8.9e+2 (55 ... ∞)	4.0 (3.1 ... 4.7)		
ACCESS-CM2	41 ˚C	5.9 (3.7 ... 13)	1.2 (0.84 ... 1.5)	2.0 (1.7 ... 2.4)	1.4 (1.2 ... 1.6)
CMCC-ESM2	38 ˚C	3.6 (1.9 ... 8.0)	0.80 (0.41 ... 1.2)	1.9 (1.7 ... 2.2)	1.1 (0.85 ... 1.2)
EC-Earth3	40 ˚C	2.9 (1.8 ... 4.5)	0.68 (0.33 ... 1.0)	1.8 (1.6 ... 2.0)	0.76 (0.59 ... 0.95)
EC-Earth3-Veg	41 ˚C	4.3 (2.8 ... 7.2)	0.90 (0.61 ... 1.2)	1.8 (1.6 ... 2.1)	0.88 (0.68 ... 1.1)
EC-Earth3-Veg-LR	40 ˚C	3.5 (2.1 ... 6.8)	0.84 (0.46 ... 1.2)	1.9 (1.6 ... 2.2)	1.1 (0.83 ... 1.3)
FGOALS-g3	42 ˚C	16 (7.0 ... 3.2e+2)	1.2 (0.86 ... 1.6)	2.0 (1.6 ... 2.4)	1.2 (1.0 ... 1.4)
INM-CM4-8	38 ˚C	1.3e+2 (28 ... ∞)	1.4 (1.1 ... 1.8)	2.0 (1.7 ... 2.4)	1.3 (1.1 ... 1.4)
MPI-ESM1-2-HR	41 ˚C	1.7 (0.94 ... 3.2)	0.43 (-0.050 ... 0.93)	1.6 (1.4 ... 1.8)	0.72 (0.32 ... 1.1)
NorESM2-MM	38 ˚C	14 (4.8 ... 55)	1.5 (0.88 ... 2.1)	2.0 (1.6 ... 2.4)	1.6 (1.3 ... 2.0)

6 Hazard synthesis

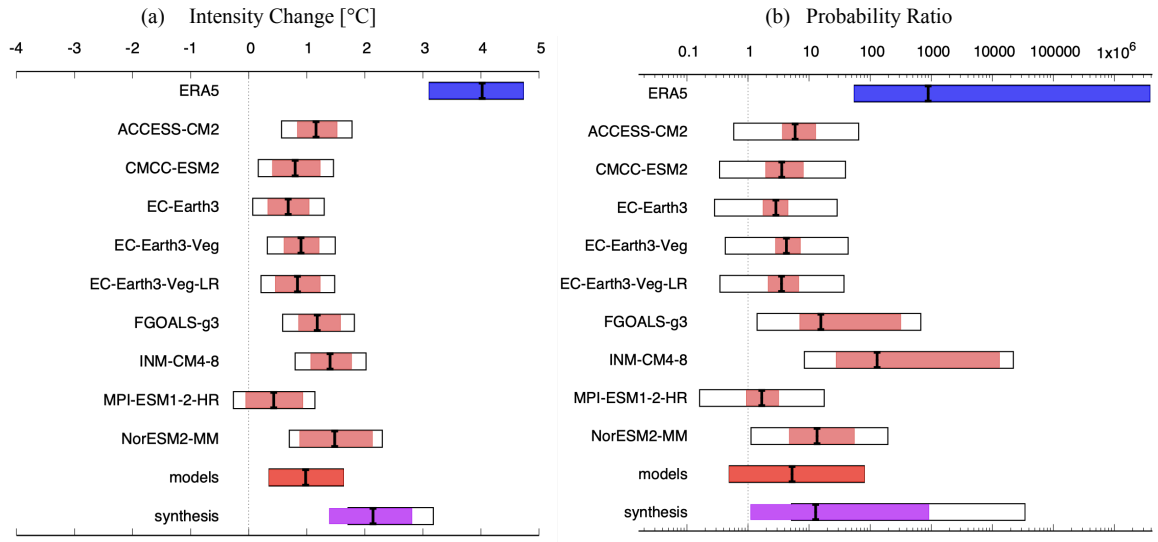

Figure 6.1. Synthesis of (left) intensity changes and (right) probability ratios when comparing the return period and magnitudes of TX7x in the South Sudan study area between the current climate and a 1.3°C cooler climate.

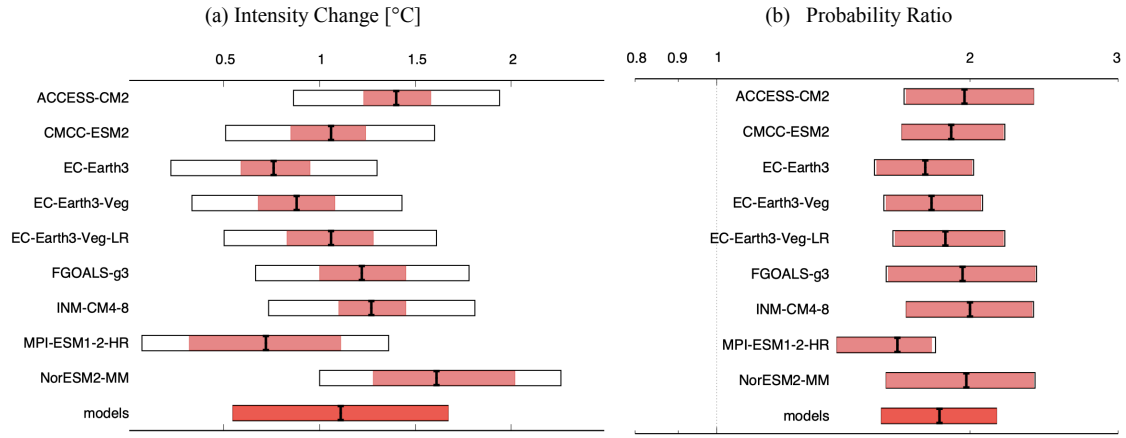

Figure 6.2. Synthesis of (left) intensity changes and (right) probability ratios when comparing the return period and magnitudes of TX7x in the South Sudan study area between the current climate and a 1.3°C warmer climate (that is, a climate that is 2.6C warmer than preindustrial).

For the event definitions described above, TX7x over the South Sudan region, we evaluate the influence of anthropogenic climate change on the events by calculating the probability ratio as well as the change in intensity using observations and climate models. Models which do not pass the evaluation described above (section 4) are excluded from the analysis. The aim is to synthesise results from models that pass the evaluation along with the observations-based products, to give an overarching attribution statement.

Figures 6.1-6.2 show the changes in probability and intensity for the observations (blue) and models (red). Before combining the observations and model results into a synthesised assessment, a term to account for intermodel spread is added (in quadrature) to the natural variability of the models. This is shown in the figures as white boxes around the light red bars. The bright red bar shows the model average, consisting of a weighted mean using the (uncorrelated) uncertainties due to natural variability plus the term representing intermodel spread (i.e., the inverse square of the white bars).

Observation-based products and models are combined into a single result in two ways. Firstly, we neglect common model uncertainties beyond the intermodel spread that is depicted by the model average, and compute the weighted average of models (dark red bar) and observations (dark blue bar): this is indicated by the magenta bar. As, due to common model uncertainties, model uncertainty can be larger than the intermodel spread, secondly, we also show the more conservative estimate of an unweighted, direct average of observations (dark blue bar) and models (dark red bar) contributing 50% each, indicated by the white box around the magenta bar in the synthesis figures.

Examining the changes that have occurred in the historical period, between a 1.3°C cooler world and now, for observations, 7-day heatwaves in the study region have increased in intensity by about 4°C (95% CI: 3.1 to 4.7 °C), as reported in Section 3 and depicted by the blue bar in Figure 6.1(a). The synthesized model results (bright red bar) show a much lower yet also positive change in intensity, of about 1°C (95% CI: 0.4-1.6 °C). All individual model intensity change results are systematically lower than for ERA5, with no overlap of the 95% confidence intervals. This is indicative of a systematic model underestimation of the trend in heatwave intensity, which is seen in other parts of the world, for example, Europe (van Oldenborgh et al., 2022, Schumacher et al., 2022). On the other hand, the observed time series shows decadal variability (Figure 3.1(a), green line), which can have an influence on the trend (e.g. a positive influence when starting with a low phase and ending in a high phase) especially when the time series is short, however it is clear that the trend is stronger than this effect (see Figure 3.1(a), and the 95% CI in Figure 6.1(a) which represents the spread due to interannual variability). The formal synthesis of observations with model results (weighted and unweighted) is shown in Figure 6.1, but due to the gap between the observations and model results, we cannot place high confidence in the best estimate (around 2°C) or the uncertainty around it, which is likely too small as we cannot directly include the common model uncertainty. We are confident that the change is positive and greater than that shown by the model synthesis. The synthesized best estimate of 2°C is even likely on the conservative side, with no conclusive explanation other than climate change for the much larger observed trend. For a future climate that is 1.3°C warmer than now, models indicate another degree of increase in TX7x magnitude, so the intensity trend is projected to linearly continue increasing with global warming. As the model trend was underestimated for the past period, we expect this to be an underestimation as well.

For the probability ratio, observations and models both show positive changes toward more frequent heatwaves but there is again a discrepancy in the magnitude of change between observations and models. Observations show a much larger factor increase than models in the frequency of 7-day heatwaves in the study region between a 1.3°C cooler world and now, with best estimates of around 900 and 5 respectively. The confidence intervals are larger than for intensity change and there is a small overlap, rather than a gap between the bright blue and bright red bar (Figure 6.1b). There are also two individual models that show larger overlap with the observational results. Since climate models underestimate the increase in heat found in observations, we can again only give a conservative estimate of the influence of human-induced climate change on the probability ratio when combining observations and models. The weighted synthesis gives a best estimate factor change in frequency of about 10 but with much higher upper bounds. The future projections show a continuation of this increase in heatwave frequency.

In summary, we communicate a conservative probability ratio of at least 10 and an increase in intensity of at least 2°C, whereby 'at least' refers to the best estimate of these synthesised metrics and not to the much lower lower bound of the confidence interval.

Data		GMST	
		Probability ratio (95% CI)	**Intensity change (%) (95% CI)**
Observations	**Past-Present**	892.89 (55 - inf)	4.024 (3.105 - 4.732)
Models		5.28 (0.494 - 80.4)	0.98 (0.351 - 1.63)
Synthesis		Weighted: 12.8 (1.11 to 913).	Weighted: 2.14 (1.39 - 2.81).
Models only	**Present-Future**	1.84 (1.57 - 2.15)	1.11 (0.548 - 1.67)

Table 6.1: Summary of Probability ratio and intensity change results for TX7x in the study region, presented in Figs 6.1 and 6.2. Statistically significant increases in probability and intensity are highlighted in dark orange, while non-significant increases are highlighted in light orange.

7 Vulnerability and Exposure

Extreme heat has increasingly become a defining feature of climate change, with profound and unequal consequences across different segments of society. In South Sudan, where structural inequalities persist, gender plays an essential role in shaping vulnerability, exposure, and coping capacity to extreme heat events. Beyond gender, other marginalized groups, including people with disabilities, older adults, and children face distinct challenges in extreme heat (UNHCR, 2022; HelpAge International, 2021). Limited mobility can hinder access to cooling spaces, and caregivers - most women - often struggle to protect dependents from heat exposure while managing their own risks. Women in the country face systemic challenges, including high maternal mortality, limited financial inclusion (only 4.2% of women have a bank account), and a vast burden of precarious employment in the informal sector (94.2% of women) (World Bank Group, n.d.). These intersecting vulnerabilities compound the risks heatwaves pose, affecting women's health, economic stability, and overall resilience.

Protracted conflict exacerbates impacts by limiting access to essential resources, such as water and healthcare, while displacement and insecurity force vulnerable populations into overcrowded, poorly ventilated shelters (Caso et al., 2023). Further, women and girls, who are already disproportionately affected by conflict and displacement, face compounding risks as they are often responsible for securing water and fuelwood - tasks that expose them to both extreme heat and heightened threats of gender-based violence (UN Women, 2024).

The 2024 and 2025 heatwaves in South Sudan illustrate the wide-ranging consequences of extreme heat. The 2024 heatwave, occurring in mid-March, recorded higher peak temperatures, while the 2025 event struck earlier in February, raising concerns that extreme heat events are intensifying and shifting seasonally. In addition to two-week school closures, the 2025 event caused an average of 12 student collapses daily in Juba (Euro News, 2025), prompting reduced public working hours (teleSUR, 2025). Both heatwaves heightened risks of early marriage, child labor, and armed group recruitment due to education disruptions (Save the Children, 2025). In displacement settings, the risks were amplified, as gender-segregated shelters often lack ventilation, while cultural taboos may prevent women and girls from seeking cooling relief, even if available (World Bank & UNHCR, 2021). Overcrowding further increases exposure to extreme heat, disproportionately affected displaced women and children (World Bank & UNHCR, 2021). They also exposed infrastructure weaknesses, with many schools lacking electricity or cooling systems (Machol, 2025). Moreover, much of the country's infrastructure, including schools and homes, relies on iron sheet roofs, which absorb and retain heat, exacerbating indoor temperatures and increasing the risk of heat stress.

During hotter months, women tend to wear lighter clothing within the boundaries of cultural expectations, which may provide some relief (Domínguez-Amarillo et al., 2021). Further, gender norms and responsibilities, such as caregiving, water collection, and agricultural labor, place women at greater risk of heat-related stress (Bérenger & Verdier-Chouchane, 2015; Munene & Wambiya, 2018; World Bank Group, n.d.). Water collection and firewood gathering, often requiring long travel distances, not only expose women to extreme heat but also increase their risk of gender-based violence (GBV), particularly in areas with ongoing conflict and displacement (IOM, 2023a). By examining the ongoing extreme heat event through a gendered lens, this analysis highlights the

disproportionate impacts on women and suggests pathways for building more equitable climate resilience in the run-up to International Women's Day.

7.1 Informality and Urban Planning for Heat

Urban areas grapple with a multitude of urban vulnerabilities shaped by armed conflict, political instability and urban planning, resulting in housing shortages, informal settlements, lack of access to basic services such as water, electricity, and healthcare, and complex urban exposure due to mobility dynamics of refugees, IDPs, and migrants (UN Habitat, 2023; Lamanna, 2019).

In South Sudan, 21% of the population resides in urban areas, with a high growth rate of 5.8% annually - driven mainly by IDPs and returning migrants - highlighting the significant influence of displacement and returns post-conflict on urban development (World Bank, 2023). Heat risks in displacement camps are particularly acute, as many shelters are overcrowded and poorly ventilated, and cultural taboos may limit women's ability to seek cooling relief (MSF, 2024; ICAN, 2024). In Juba, built-up areas tripled between 2000-2010 and grew an additional 75% by 2020, creating a dense city center (UN Habitat, 2021). Consequently, due to a mix of these factors, 94% live in informal settlements, one of the highest proportions in the world (UN Habitat, 2022).

The Urban Heat Island (UHI) effect increases temperatures in informal settlements and has been linked to increased mortality and morbidity in East Africa (Kimutai et al., 2022), although no data exist for South Sudan (Lamanna, 2019). UHI is linked to increased day and nighttime temperatures in the capital Juba. However, a high mix of building properties, complex city landscapes and close water proximity to the Nile, points to smaller micro UHI that are difficult to identify (Garuma, 2023). This can be observed in areas of intra block informality and makeshift structures, with iron sheets (See picture below), with limited cooling/ventilation, common in Juba and including public spaces like schools (Hindustan Times, 2025). Furthermore, IDPs are likely more exposed, since some camp structures and materials are particularly susceptible to heat and IDPs account for 15% of the population in Juba (Amarillo et al., 2021; UN Habitat, 2023).

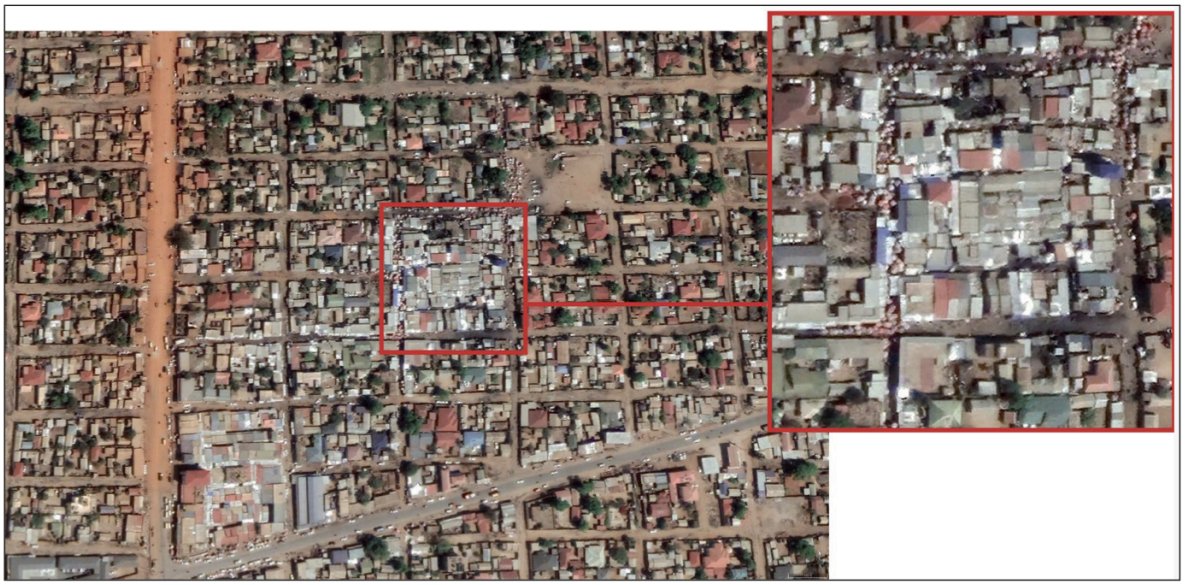

Intra-block developments in Juba depict congestion and lack of order and some blocks depict morphological characteristics that resemble slum. Source: Google Earth, 2020

Picture and caption retrieved from (UN Habitat, 2021)

Coping mechanisms, such as hydration and access to cooler spaces, are constrained in Juba. Green spaces cover less than 1% of urban areas (UN Habitat, 2023), electricity access is 15% (World Bank, 2022), one-third of residents lack drinking water and WASH facilities (WHO/UNICEF, 2022). Lacking access to air conditioning, many, particularly women, are forced to sleep outdoors during extreme heat events. This practice increases exposure to security risks, including heightened vulnerability to sexual violence, which remains prevalent due to high levels of criminality and the presence of organized gangs in South Sudan. Moreover, community halls that could become cooling centers often lack electricity or water supplies (UN Habitat, 2021).

Further exposure and vulnerabilities arise from urban livelihoods. Most people rely on various economic activities, with the urban poor particularly exposed to heat through jobs like agriculture, construction, and unpaid domestic work (Von der Goltz & Harborne, 2021; Kurcz, 2021). Within urban livelihoods, women face compounded vulnerabilities due to gender roles, lack of economic opportunities, lower employment and prolonged heat exposure during tasks like water fetching or household chores in hot indoor environments (Von der Goltz & Harborne, 2021; Kurcz, 2021; African Development Bank, 2023). Additionally, women-headed households are more vulnerable, making them both caretakers and primary earners, reliant on informal employment (Kurcz, 2021; African Development Bank, 2023).

The challenges posed by extreme heat in urban settings are further intensified in displacement contexts, where infrastructure is even more fragile and living conditions more precarious.

7.2 Disaster Displacement

East African countries recorded large numbers of displaced people between 2009 and 2023, with South Sudan and Somalia at the forefront of disaster and conflict-related and protracted displacement. At the end of 2023, South Sudan had 1.1 million internally displaced people making it one of the top ten countries most affected by conflict-related displacement (IDMC, 2024). Heat-related resource competition could also exacerbate existing tensions, particularly in displacement camps and water-scarce regions, where armed groups may exploit scarcity for recruitment or control (IOM, 2023b).

Ajuong Thok refugee camp shelters over 40,000 people, most of whom are women. The camp illustrates the importance of shelter design in mitigating heat risk. Studies suggest that UNHCR's Tukul Shelters offer greater stability and slower heat accumulation, factors that could play a role in improving heat resilience for displaced populations (Domínguez-Amarillo et al., 2021).

In 2020, riverine flooding of the White Nile displaced 960,000 people in Sudan, South Sudan and Uganda (FAO, 2020). The situation was compounded by difficulties to recover from flooding and the 2019 elevated river levels. Roads and houses were still being rebuilt when the flood hit, leading to repeated displacement and delays in humanitarian aid delivery (JRS, 2020). Leaving populations vulnerable and unable to cope with previous floods, the country experienced a combination of floods and conflict in 2022 when non-state armed groups took advantage of the situation. In the Unity and Jonglei states, these groups increased the checkpoints along the White Nile, looted aid convoys and extorted aid organisations (ACAPS, 2025). A similar overlap of the country hosting internally

displaced from flood and conflict happened in 2023 (IOM DTM, 2022). As a result, South Sudan's policy focuses on peacebuilding and reconciliation, facilitating return migration and integration of displaced populations (Republic of South Sudan, 2022). In particular, the Revised National Development Strategy 2021-2024 aims to renovate schools damaged by conflict and facilitate displaced children's return and reintegration (Republic of South Sudan, 2017).

Displacement amplifies existing health risks, particularly for those with heightened physiological vulnerability, such as pregnant women and newborns.

7.3 Maternal and Neonatal Health

Women undergoing anatomical, physiologic and socio-cultural changes during pregnancy and childbirth, and their newborns, have a higher susceptibility to high temperatures (Chersich et al., 2022). Traditional birth attendants (TBAs), who assist many births outside formal healthcare facilities, often lack training in heat-stress management and operate with limited resources, such as hydration supplies and cooling systems (Chersich et al., 2022). This further endangers maternal and neonatal health, increasing risks of heat-induced complications (Chersich et al., 2022). A synthesis of 198 research studies across 66 countries found that heat exposure was linked to an increase in preterm birth, increased risk of stillbirth, congenital anomalies, and gestational diabetes (Lakhoo et al., 2024). While there are studies that have documented heat impacts on pregnancy outcomes in Ethiopia, South Africa and Uganda, there is a gap in research that documents this linkage in South Sudan (Chersich et al., 2022). Studies in neighbouring countries have shown that heat waves can be associated with more low birth weight births, increased cesarean sections (Brimicombe et al., 2025), and impacts on breastfeeding and sleeping conditions for mothers (Lusambili et al., 2024).

South Sudan has one of the world's highest maternal mortality rates at 1,223 deaths per 100,00 live births (WHO, 2023). Researchers suggest that this is linked to a variety of reasons, including a poor health system with limited accessibility and utilization. For example, access to services for antenatal care is particularly low in Juba county, with only 58.7% of pregnant women attending 4 or more visits in 2019 (UN Habitat, 2021). This is especially a risk for people living in informal housing in urban areas that experience the urban heat island effect, doubly increasing the exposure of pregnant women to high temperature, especially if they give birth at home (Chersich et al., 2022).

Neonates and infants are uniquely vulnerable to heat stress due to their lower ability to dissipate heat and thermoregulate (Nakstad et al., 2022). They also depend on others for hydration and to avoid heat exposure, making them especially vulnerable.

Beyond direct health effects, extreme heat also threatens livelihoods, especially for those engaged in physically demanding, outdoor, and/or domestic work.

7.4 Workplace Heat Stress and Livelihood Vulnerabilities

Recent temperature spikes pose severe health threats, particularly for individuals engaged in outdoor labor or working in environments without adequate cooling measures. Agriculture, a sector employing 59% of the population, is a critical area of concern (World Bank, 2025a). Women, who make up 73% of all employed women in the agricultural workforce (compared to 46% of all employed men), are

particularly exposed to heat-related risks (World Bank, 2025b). While the current dry hot season generally sees reduced agricultural activity, certain tasks, such as irrigated market gardening, continue (WFP, 2020). Community gardens, where women play a significant role (FAO, 2022), may have been affected by the extreme temperatures, heightening their vulnerability to heat stress. Although no direct impacts have been officially recorded, the risks remain significant, particularly for those with prolonged exposure without shade, hydration, or cooling options.

Beyond agriculture, domestic work presents additional risks, particularly for women who dedicate approximately 60% of their time to unpaid care duties (UN Women, 2024). Activities such as cooking over open fires, cleaning, and carrying water involve sustained physical exertion, increasing the likelihood of dehydration and heat exhaustion. The absence of cooling measures in many households further compounds the risks, partly because South Sudan has the lowest electricity access in the world (UNICEF, 2018).

The impacts of heat exposure compound for women balancing agricultural labor (or another occupation with high heat exposure, such as street vending or manufacturing) with domestic responsibilities. This sustained heat exposure can have serious long-term health effects, including cardiovascular strain, kidney damage, and increased vulnerability to heat exhaustion and heat stroke.

The ability to manage heat risks associated with work is closely tied to broader access to essential services, including safe and reliable water, electricity, and healthcare.

7.5 Water, Electricity, and Health Systems

South Sudan's urban infrastructure and basic services have not kept pace with its growing urban population. The legacy of armed conflict has led to a severe shortage of housing, healthcare, water, and electricity in major cities, exacerbating the challenges faced by marginalised groups, particularly women and girls (UN Habitat, 2023). The country's fragile healthcare system, coupled with inadequate water and electricity supply, raises concerns about the ability of these systems to expand and withstand increasing pressures, particularly during extreme climate events such as heatwaves. In 2024, the system transitioned to the World Bank-funded Health System Transition Program following the discontinuation of the Health Pool Fund, which had previously supported most health facilities (World Bank, 2024). This shift has led to a reduction in functional health facilities, many now managed by under-resourced partners (USAID, 2023).

The low rate of formal built infrastructure, including roads, public transportation, and adequate facilities significantly hinders transportation of food and access to essential services (Mercy Corps, 2019). Only 40% of the population has access to safe drinking water (World Bank, 2022), significantly increasing the risk of worsened country-wide cholera outbreak starting in October 2024 (WFP, 2025). The ongoing heatwave further exacerbates the crisis by accelerating dehydration, placing additional stress on already scarce water resources, and complicating disease prevention efforts. Additionally, only 7% have access to electricity, and just 10% have access to improved sanitation (World Bank, 2022). These deficiencies disproportionately affect women, who are responsible for collecting water in 84.9% of households, compared to just 5.8% of men (Mai, Jok, & Tiitmamer, 2018). The long distances women and girls travel to fetch water and firewood not only

exposes them to security risks including rape and violence, but also limit their time for education, community engagement, and advocacy for their needs (Mohammed & Laki, 2025).

The recent heatwave further strained essential services. Many schools, built from iron sheets and lacking electricity to power cooling systems, provide little protection from extreme heat. In some cases, building materials can exacerbate the heat, making indoor temperatures higher than those outdoors. The Environment Minister, Josephine Napwon Cosmos, advised residents to stay indoors and drink water as temperatures soared to 42°C (Arab News, 2025). However, staying indoors is not an option for many, and access to adequate drinking water is inconsistent. Schools outside Juba, particularly those in rural areas, are congested, underfunded, and lack cooling infrastructure, leaving children at risk of heat exhaustion and heatstroke.

South Sudan's nascent healthcare system, already grappling with limited financing and worker shortages, is expected to face significant strain due to the ongoing heatwave (Dahir, 2025). The local government-led service delivery has been limited with about 70% of South Sudanese lacking access to adequate medical services (World Bank, 2022). The shortage of medical professionals, infrastructure, and essential supplies further diminishes the country's ability to respond effectively to heat-related illnesses, compounding existing public health challenges.

Malnutrition remains a critical concern, around 860,000 children under five are acutely malnourished (UNICEF, 2019). Malnutrition is exacerbated by climate-induced shocks such as floods, droughts and extreme heat, as well as political and communal violence, which lead to crop failures, famine, and the looting of assets, including livestock and land (Mai, Jok & Tiitmamer, 2018). Households headed by women have been found to have higher proportions of malnourished children, indicating gendered economic and social vulnerabilities. During a heatwave, malnourished children are particularly at risk, as their weakened immune systems make them more susceptible to dehydration and heat-related illnesses, further exacerbating the crisis. Health-related challenges are further exacerbated by the population's limited proximity to medical facilities and restricted access to clean water and sanitation services.

Gaps in infrastructure and services highlight the need for stronger governance and coordinated heat adaptation measures.

7.6 Heat Risk Governance

In February 2025, extreme temperatures affected several regions of East Africa, including South Sudan (ICPAC, 2025). In response to the forecasted above-average temperatures, the South Sudan Meteorological Service (SSMS) issued early warnings for extreme heat stress in Juba and its surrounding areas, urging precautions to safeguard public health. Parents were advised by Minister of Health Ayaa Benjamin Warille to keep their children indoors (DW, 2025). She also stressed the importance of staying hydrated, urging the public to avoid outdoor activities during peak heat periods. As a measure to reduce risk, authorities implemented a two-week nationwide school closure - mirroring actions taken during the same period last year (Dahir, 2024) - after reports of a daily average of 12 students collapsing from heat stroke in Juba (Machol, 2025). Education workers have called on the government to consider changing the school calendar so that schools close in February and reopen in April when temperatures decrease (DW, 2025). While this intervention aims to reduce immediate exposure, it also disrupts education, posing long-term risks, particularly for girls.

Prolonged school closures increase the likelihood of learning losses, reinforce gendered household expectations, and heighten risks of early marriage, making school return more difficult for girls (Save the Children, 2025; UNICEF, 2021).

Structural challenges further limit heat risk management. Political instability and conflict have constrained government resources, leaving heat action planning remains underdeveloped. Additionally, urban development plans are scarce. While the National Adaptation Plan acknowledges heat impacts in urban areas (South Sudan Ministry of Environment and Forestry, 2021), heat is not currently integrated into urban development plans. Current urban planning and risk mitigation efforts primarily focus on floods and droughts, with limited attention to heat-related risks (UN Habitat, 2023). Importantly, decision-making on heat response and urban planning is often male-dominated, leaving women, youth, and IDPs underrepresented.

V&E conclusions

The increasing frequency and intensity of early-season extreme heat events in South Sudan pose escalating risks to vulnerable populations. The compounding and cascading effect of disasters in conflict settings include displacement, fragile healthcare systems, informal labor, and weak infrastructure which further limits adaptive capacity, particularly for women, children, older adults, and low-income workers.

While large-scale adaptation remains challenging due to existing development constraints, in both rural and urban areas, there are opportunities for incremental action to reduce risks and strengthen resilience. It is critical to ensure safe access to water points and cooling centers, particularly in displacement camps and informal settlements. The structure and materials used for temporary shelters in displacement camps can be improved to account for extreme heat. Expanding targeted cash transfer programs, climate-smart agricultural training for women farmers, and support for women-led cooperatives in heat-exposed sectors can help build economic resilience. Community-driven strategies such as women-led cooling projects, grassroots early warning systems, and participatory urban design for heat-sensitive infrastructure offer locally viable solutions. Strengthening impact-based early warning systems, such as the Early Warning for IGAD (EW4IGAD) initiative, is also critical, to provide advanced warning of possible heat impacts. However, ensuring localised, impact-based messaging remains a challenge, particularly for remote, conflict-affected and displaced communities. Improving last-mile dissemination and integrating traditional knowledge into warning systems could enhance early and anticipatory actions. As education is disrupted during these intense heat weeks, efforts must be taken to bring all children back to school. Changing the hours of school to cooler time of day, retrofitting passive cooling options into school buildings, and promoting heat safety and first aid can all help to reduce the impacts on children.

Integrating heat risk management into broader development planning requires, for example, to expand access to water and cooling, and improve heat-sensitive urban design in displacement settings. Conflict-sensitive approaches, such as ensuring action for reducing risks of gender-based violence, and access to relief, will be key. While large-scale investments remain a challenge, targeted measures can still strengthen coping capacities against escalating extreme heat to reduce disruptions to livelihoods, deepened food insecurity, and additional strain on essential services.

Data availability

All time series used in the attribution analysis are available via the Climate Explorer.

References

All references are given as hyperlinks in the text.

Appendix

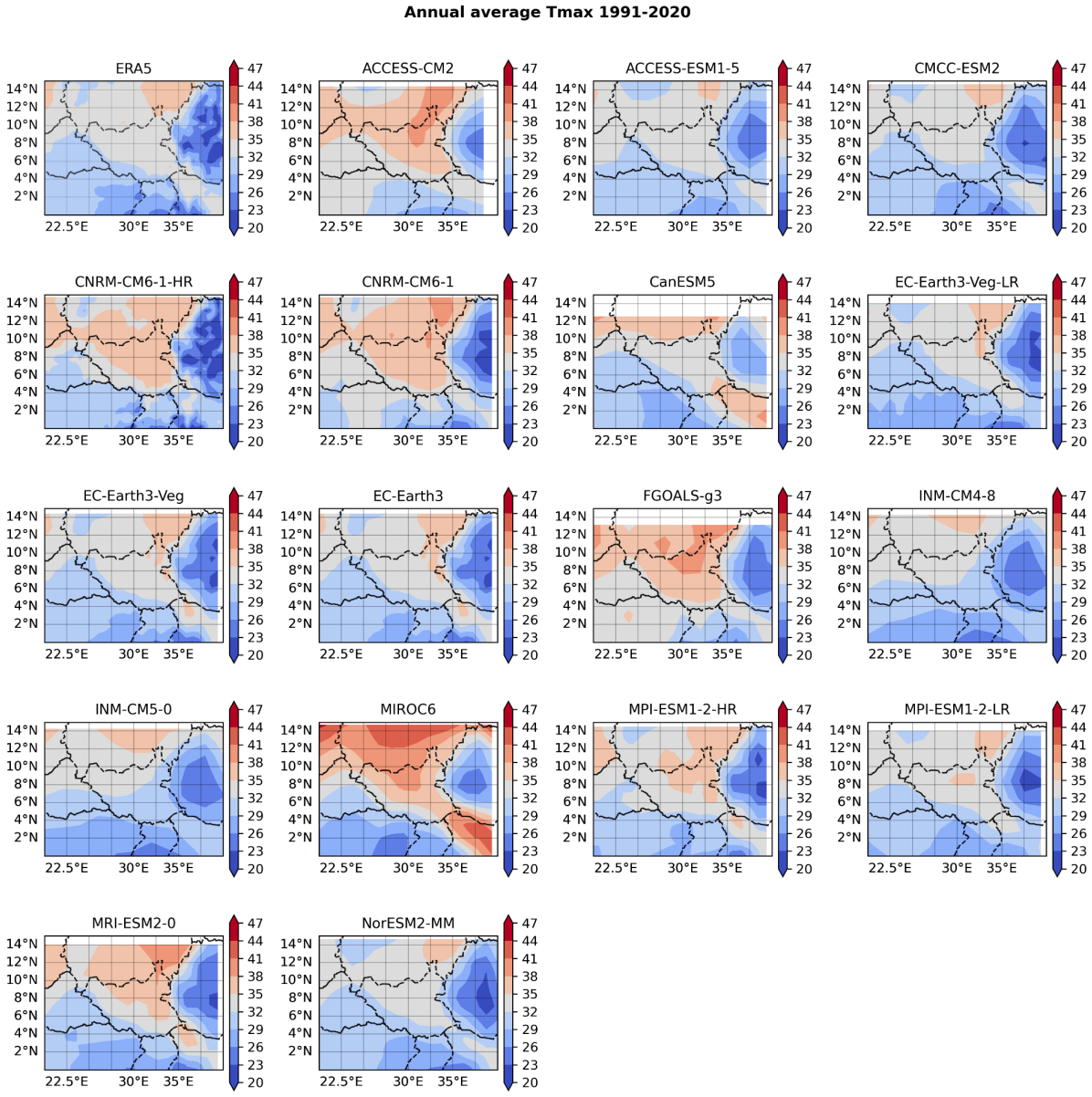

Figure A1. Tmax averaged for January-December over a climatological period of 1991-2020 of ERA5 and CMIP6 models. Borders shown are generated using a standard plotting package and do not imply official endorsement nor political opinion on included territories.

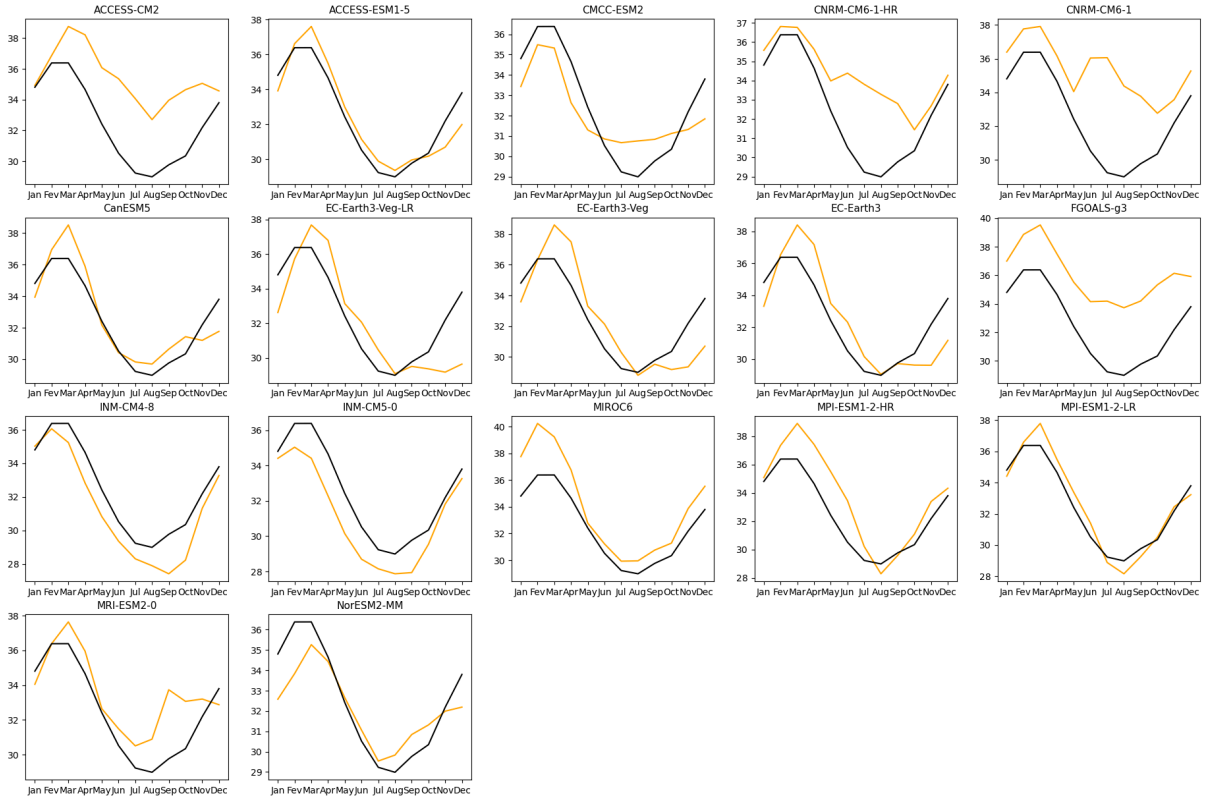

Figure A2. Seasonal cycle of Tmax over a climatological period of 1991-2020 of ERA5 and CMIP6 models over the study area (blue box of Figure 1b).